

NUMERICAL INVESTIGATION OF SUBSONIC RAREFIED FLOWS USING DSMC-IP METHODS

Young Jae Choi*, Oh Joon Kwon*

*Korea Advanced Institute of Science and Technology (KAIST)

Keywords: *subsonic rarified gas flows, DSMC, information preservation (IP), Couette flows*

Abstract

In the present study, to investigate the characteristics of subsonic rarefied gas flows, simulations of Couette flows, micro-channel flows, and airfoil flows were performed using a direct simulation Monte-Carlo (DSMC) method based on unstructured meshes. However, it is known that the DSMC method makes relatively large statistical scatter for low speed, micro-scale flows due to the small variation of velocity and temperature. To overcome these statistical errors in the DSMC method, the information preservation (IP) method known that it can reduce the scatter problems was also developed based on the DSMC method.

Firstly, to verify the DSMC and the IP solver, two cases of the micro-channel flows were calculated. Since the micro-channel flows are based on pressure-driven flows, the pressure conditions at inlet and exit are necessary. The pressure ratio of inlet to exit for the case 1 was about 3, and for the case 2, it was about 4. $5\mu\text{m} \times 1\mu\text{m}$ micro-channel was used. The inlet gas temperature and wall temperature were both 300 K. The DSMC and IP calculations were compared with the other researchers' DSMC results. The velocity profiles at the 2/3 section of the channel for the two cases agreed well with the other researchers' results. In addition, the normalized slip velocity distributions on the wall and the pressure distributions along the centerline also agreed well with the other researchers' results. Furthermore, it was shown that the statistical scatter errors were reduced in the IP results.

Secondly, two types of Couette flows were considered. One is the flows that have temperature differences between two plates, and

the other is the flows that have moving plates. For the first Couette flows, the temperature of 373K was used for the upper plate, and of 173K for lower plate. For the second Couette flows, the upper plate is moving at 300m/s, and the temperature of 273K was used for both two plates. All simulations of Couette flows were conducted from near-continuum to free-molecular regimes. From both Couette flow simulations, it was found that the temperature jump and the velocity slip occurred on the plate surface. In addition, it was also shown that the temperature and the velocity differences between the plate and the gas became larger as the flow fields became more rarefied.

Lastly, flow simulations around a NACA0012 airfoil were conducted. The freestream Mach number of 0.8 was used, and the Knudsen number of 0.014 was considered. It was observed that more clear contours were obtained from the IP method than the DSMC method, since the statistical scatter error was reduced by the IP method. In addition, it was found that the velocity slip on the airfoil surface occurred due to the effects of the rarefied atmospheric environment.

1 Introduction

Over the past decades, interest in the development of micro-scale vehicles such as micro-electro-mechanical systems (MEMS) has been significantly improved. Since these micro-scale structures are experienced through the subsonic rarefied flows ranging from the near-continuum to the free-molecular regimes, methods able to analyze those flow regimes are necessary.

Flow regimes are generally classified by the Knudsen number (Kn), which is defined by the ratio of a mean free path to a characteristic length. The continuum regime is commonly called the area where the Knudsen number is less than 0.01. The rarefied gas flow regime is composed of the slip, the transition, and the free-molecular regime. The slip and transition regimes are in the Knudsen number range 0.01 to 0.1 and 0.1 to 10, respectively. If the Knudsen number is greater than 10, it is usually called as the free-molecular regime. It is known that rarefied phenomena such as velocity slip and temperature jump occur on the body surfaces when the Knudsen number is greater than 0.01.

The DSMC method is well known for one of the most popular methods for rarefied gas flows [1]. The DSMC method is performed by simulating particles movement depending on the kinetic theory. However, it is known that the DSMC method makes relatively large statistical scatter for low speed, micro-scale flows due to the small variation of velocity and temperature [2]. To overcome these statistical errors in the DSMC simulations, the IP method was proposed by Fan and Shen [3] at first. The IP method can reduce the statistical scatter by preserving the macroscopic information of the flow in the particles and the computational cells simulated in the DSMC method.

In the present study, to investigate the characteristics of subsonic rarefied gas flows, the DSMC solver based on unstructured meshes was used, and the IP method solver was developed to reduce the statistical scatter errors of the DSMC method. For verification of the DSMC and the IP solver, flow simulations of micro-channels were conducted at first. The results of the simulations were compared with those of the simulations assessed by other researchers' [4]. To further investigate the characteristics of subsonic rarefied gas flows, thermal and slip Couette flows were considered. All simulations of Couette flows were conducted from near-continuum to free-molecular regimes. Additionally, Flow simulations around a NACA0012 airfoil were conducted using the DSMC and IP solver.

2 Numerical Methods

2.1 Direct Simulation Monte-Carlo (DSMC)

The fundamental concept of the DSMC method is to obtain the flow field properties (e.g. density, velocity, temperature, and pressure) by sampling the information of simulated particles. A simulated particle represents an enormous number of real molecules, and the information of the particles is composed of position, velocity, and chemical species. The position of particles is determined by the moving distance of particles during Δt by using the velocity components of particles. The velocity of the particles is comprised of the mean molecular velocity and the thermal velocity. They represent the macroscopic velocity and the velocity scatter, respectively, since the thermal velocity is calculated by using random number functions with temperature.

Three main components of the overall procedure of the DSMC method are the movement of particles, the collisions between particles, and the particles data sampling. In the movement step, particles can collide with the solid wall boundary condition, and then the velocity of particles is determined by a reflection model. In the collisions step, translational energy and internal energy of particles are decided by an energy exchange model. In the sampling step, the macroscopic information is calculated statistically by the sampled microscopic information.

To simulate thermal Couette flow at several Knudsen numbers, the DSMC solver based on unstructured meshes was utilized. The boundary conditions were composed of freestream, symmetric, solid wall, vacuum, plume, and periodic condition. Specular and diffuse reflection models were employed as the wall boundary condition. No time counter (NTC) method [1] was adopted for calculating intermolecular collisions, and the collision cross-section was computed by the variable soft sphere (VSS) model [5, 6]. The Larsen-Borgnakke (L-B) phenomenological model was used for the internal energy exchange model.

2.2 Information Preservation (IP)

To overcome the statistical scatter problems in the DSMC method, particularly, for systems in which the flow speed is much smaller than the molecular speed, the IP method was introduced by Fan and Shen [3] at first, and the method was further developed by Sun et al. [7].

In the present study, Sun's modified IP approach [7] was employed in the DSMC method. The macroscopic velocity components (u_i, v_i, w_i), temperature (T_i), and additional temperature term ($T_{a,i}$) were added in the particle data structure, and additional temperature term ($T_{a,c}$) was added for the cell data structure. At first, the macroscopic information of the particles and cells is initialized by the ambient condition. Next, particles movements and collisions are performed by the DSMC method, and the additional temperature is changed. The macroscopic velocity and temperature of particles are updated by calculating the equations as

$$\frac{\partial}{\partial t}(\rho_c \vec{V}_i) = -\nabla p_c \quad (1)$$

$$\frac{\partial}{\partial t} \left(\frac{1}{2} \rho_c (V_i^2 + \xi R T_i) \right) = -\nabla \cdot (p_c \vec{V}_i) \quad (2)$$

where R and ξ are gas constant and degree of freedom of the gas particle, respectively. After the macroscopic information of the particles is updated, the flow properties are computed as

$$\vec{V}_f = \sum_{i=1}^{N_p} \left(\frac{\vec{V}_i}{N_p} \right) \quad (3)$$

$$T_f = \sum_{i=1}^{N_p} \left(\frac{T_i + T_{a,i}}{N_p} \right) + \frac{1}{\xi R} \left(\sum_{i=1}^{N_p} \frac{\vec{V}_i \cdot \vec{V}_i}{N_p} - \left(\sum_{i=1}^{N_p} \frac{\vec{V}_i}{N_p} \right) \cdot \left(\sum_{i=1}^{N_p} \frac{\vec{V}_i}{N_p} \right) \right) \quad (4)$$

where N_p is the number of all particles in each cell.

3 Results and Discussion

3.1 Microchannel Flows

To verify the pressure boundary condition, two cases of flow simulations of micro-channels were conducted with the same conditions calculated by Wang [4]. The pressure ratio of inlet to exit is 3 and 4, respectively, and the pure nitrogen was used for gas species. The conditions are presented in Table 1, and the configuration is depicted in Fig. 1. The size of the channel is $5\mu\text{m} \times 1\mu\text{m}$, and it is composed of 12546 triangular cells. The fully diffuse reflection model was used for the wall boundary condition.

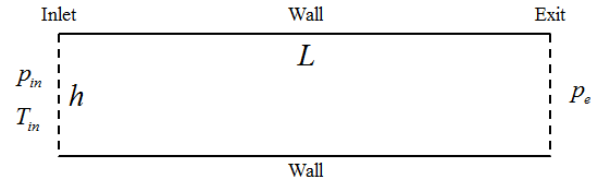


Fig. 1 Configuration of a micro-channel

Table 1 Flow conditions for micro-channel

Case #	P_{in} (Pa)	P_{ex} (Pa)	T_{in} (K)	T_w (K)
1	1.5×10^5	0.50×10^5	300	300
2	0.6×10^5	0.15×10^5	300	300

Comparison of the dimensionless velocity profiles at about 2/3 section of the channel for the three cases is shown in Fig. 2. It is shown that the velocity profiles agree well with the Wang's DSMC results [4]. As the local Knudsen number is increased, the velocity slip on the wall is also increased. Fig. 3 shows the velocity slip along the wall and the pressure drop along the centerline of the channels. It is also found that the present results are close to the Wang's results. The velocity slip on walls in the channel is increased as the local Knudsen number is increased. It is shown that the pressure between the inlet and the exit are consistently dropped according to the given conditions. As a result, it is obtained that the applied boundary conditions are well performed in the DSMC solver, and the modified DSMC

solver is appropriate for subsonic micro-channel flows.

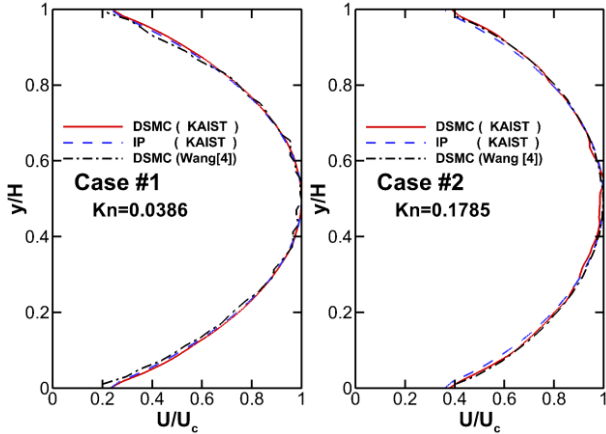


Fig. 2 Dimensionless velocity profiles at 2/3 section of the channel

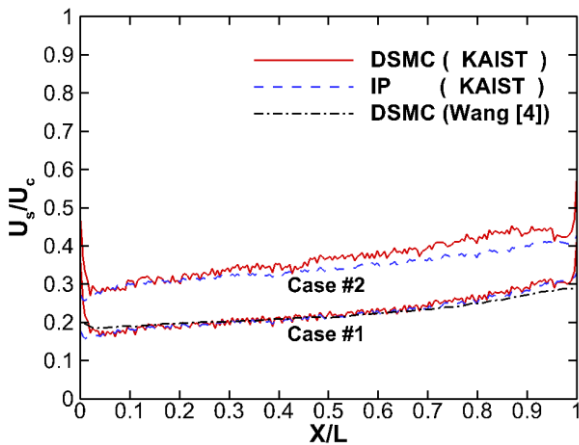


Fig. 3 Dimensionless velocity slip along the wall

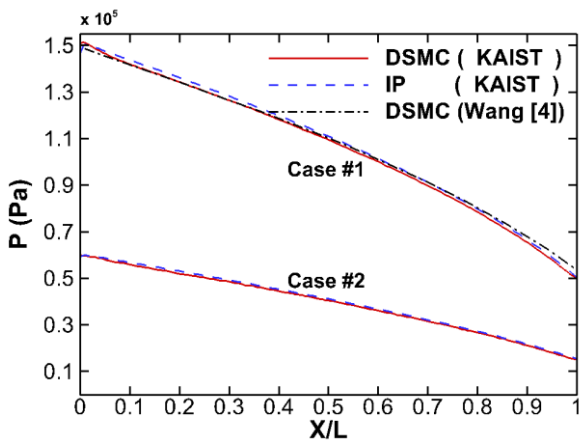


Fig. 4 Pressure distribution along the centerline

3.2 Couette Flows

For the flow simulations, two kinds of Couette flows were considered. One is the thermal Couette flows that it has a temperature difference between two plates, and the other is the velocity slip Couette flows that it has moving plates. Fig. 5 shows the schematic diagram and temperature distributions for the thermal Couette flows. Temperatures of plate 1 and 2 were set to 173 K and 373 K, respectively. Five Knudsen numbers (0.01, 0.1, 1, 10, and 100) were considered, and gas species of the flow between two plates were set to pure argon (Ar). The diffuse wall reflection model was employed as the solid wall boundary condition.

Temperature distributions between two plates are compared with the DSMC and IP calculation in Fig. 6. It is found that the IP results almost coincide with the DSMC results. It is also found that the gradient of the temperature distributions is decreased as the Knudsen number is increased, and as a result, the temperature jump on the plate surfaces is increased.

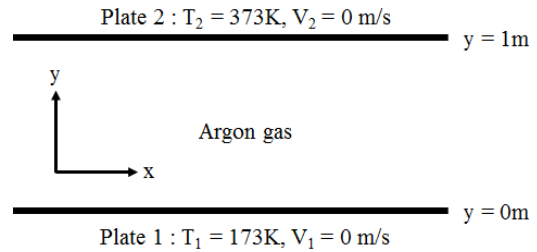


Fig. 5 Schematic diagram for thermal Couette flows

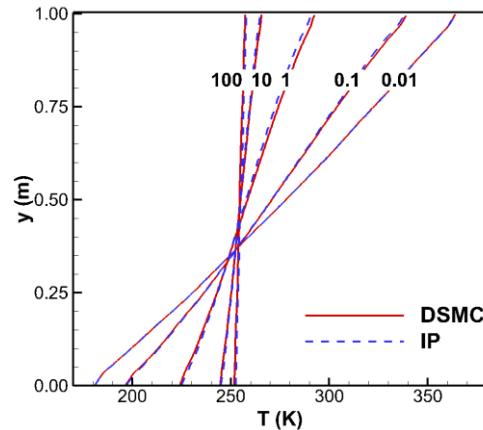


Fig. 6 Temperature distributions between two plates at different Kn

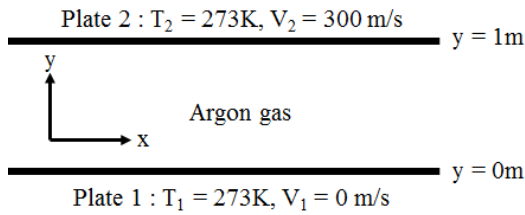


Fig. 7 Schematic diagram for velocity slip Couette flows

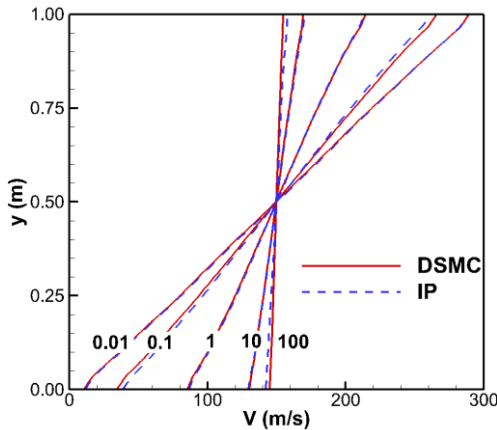


Fig. 8 Velocity distributions between two plates at different Kn

Fig. 7 shows the schematic diagram and velocity distributions for the velocity slip Couette flows. Plate 2 is moving at 300m/s. Identical conditions of the thermal Couette flows were considered. Velocity distributions between two plates are also compared with the DSMC and IP method. The IP results correspond approximately with present DSMC results. It is also found that the gradient of the velocity distributions is decreased as the Knudsen number is increased, and as a result, the velocity slip on the plate surfaces is increased.

3.3 Flow over a NACA0012 Airfoil

Flow simulations around a NACA0012 airfoil were conducted using the DSMC and IP solver. A chord length of 0.04m is used, and freestream Mach number of 0.8 is considered. The detailed flow condition is presented in Table 2, where Kn_∞ is based on the chord length.

As the computational domain is depicted in Fig. 9, meshes are clustered near the airfoil.

Table 2 Flow conditions for the airfoil

Ma_∞	Kn_∞	L_{chord} (m)	T_∞ (K)	T_w (K)
0.8	0.014	0.04	257	290

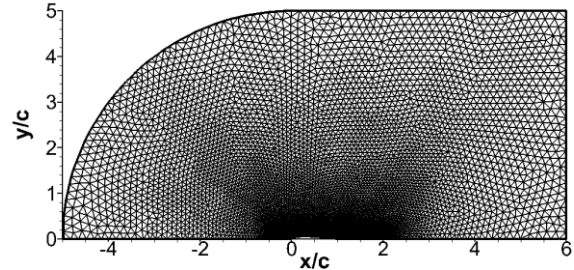


Fig. 9 Computational meshes for flow over a NACA0012 airfoil

16453 unstructured cells are used for the simulations. The airfoil surface is considered as a fully diffused wall.

Figs. 10-12 show the density, Mach number, and the pressure contours, as a result of the DSMC and IP methods. Due to the scatter, the contours in DSMC results are still rough, but the results of both two methods agree well with each other. Since the stagnation point is located at the leading edge, it is shown that high pressure and density regions are around the leading edge, whereas the Mach number is accelerated as close to the trailing edge. From the Mach number contours, it is observed that sonic regions occur as a result of the acceleration of transonic flows. However, any compressed shock waves do not appear unlike in the continuum regimes. This can be identified from the pressure coefficient distributions on the airfoil surface, as depicted in Fig. 13. Furthermore, from the flow velocity distributions on the surface, it is found that the velocity slip on the surface is captured well.

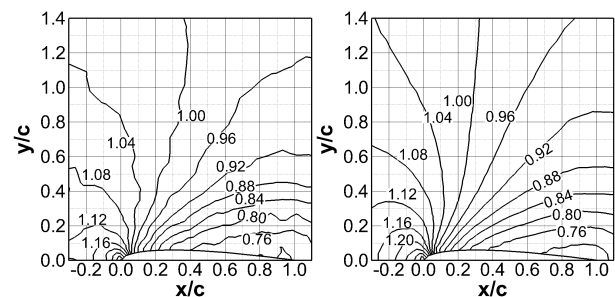


Fig. 10 Density (ρ/ρ_∞) distributions around a NACA0012 airfoil (left : DSMC, right : IP)

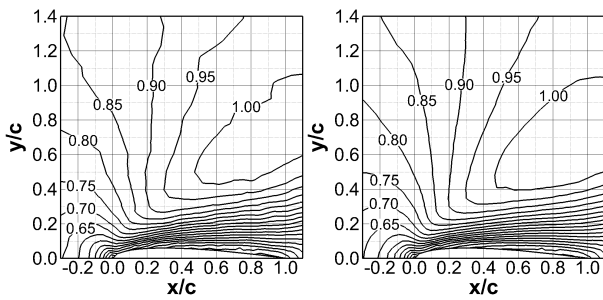


Fig. 11 Mach number distributions around a NACA0012 airfoil (left : DSMC, right : IP)

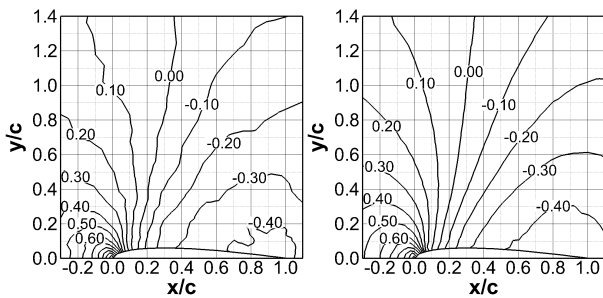


Fig. 12 Pressure (C_p) distributions around a NACA0012 airfoil (left : DSMC, right : IP)

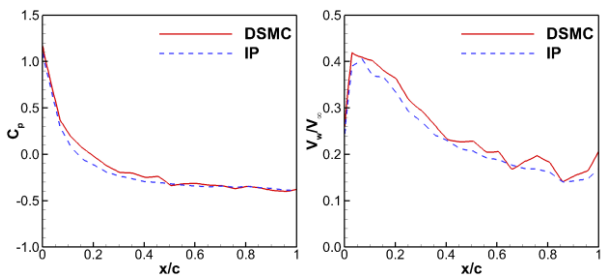


Fig. 13 Pressure (C_p) and flow velocity (V/V_∞) distributions on a NACA0012 airfoil surface (left : pressure, right : velocity slip)

4 Conclusions

In the present study, to investigate the characteristics of subsonic rarefied gas flows, the IP solver based on the DSMC solver was developed at first, because the IP method is known for reducing the statistical scatter errors in the DSMC method for low-speed rarefied flows. To verify the DSMC and the IP solver, two cases of the micro-channel flows were calculated using both DSMC and IP solver. Since the micro-channel flows are based on pressure-driven flows, the pressure boundary condition at inlet and exit was adopted. The DSMC and IP calculations were compared with

the other researchers' DSMC results. Then, the velocity profiles at the $2/3$ section of the channel for the two cases agreed well with the other researchers' results. In addition, the normalized slip velocity distributions on the wall and the pressure distributions along the centerline also agreed well with the other researchers' results. Furthermore, it was shown that the statistical scatter errors were reduced in the IP results.

As a next step, Couette flows were conducted from near-continuum to free-molecular regimes. From both Couette flow simulations, it was found that the temperature jump and the velocity slip occurred on the plate surface. In addition, it was also shown that the temperature and the velocity differences between the plate and the gas became larger as the Knudsen number became larger.

Finally, flow simulations around a NACA0012 airfoil were conducted. It was observed that more smooth contours were obtained from the IP method than the DSMC method, since the statistical scatter error was reduced by the IP method. In addition, it was found that the velocity slip on the airfoil surface occurred due to the effects of the rarefied atmospheric environment.

5 Acknowledgement

This work was supported by Grant (UD130051CD) from Agency for Defense Development (ADD) and Defense Acquisition Program Administration (DAPA).

References

- [1] Bird G. *Gas dynamics and the direct simulation of gas flows*. 1st edition, Clarendon Press, 1994.
- [2] Sun Q and Boyd I. A direct simulation method for subsonic, microscale gas flows. *Journal of computational physics*, Vol. 179, pp 400-425, 2002.
- [3] Fan J and Shen C. Statistical simulation of low-speed unidirectional flow in transition regime. *Proceedings of the 21th international symposium on rarefied gas dynamics*, pp 245-252, 1998.
- [4] Wang M and Li Z. Simulations for gas flows in microgeometries using the direct simulation Monte Carlo method. *International journal of heat and fluid flow*, Vol. 25, pp.975-985, 2004.

- [5] Koura K and Matsumoto H. Variable soft sphere molecular model for inverse-power-law of Lenard Jones potential. *Physics of fluids A*, Vol. 3, pp.2459-2465, 1991.
- [6] Koura K and Matsumoto H. Variable soft sphere molecular model for air species. *Physics of fluids A*, Vol. 4, pp.1083-1085, 1992.
- [7] Sun Q. *Information preservation method for modeling micro-scale flows*. Ph.D. dissertation, Department of aerospace engineering, University of Michigan, 2003.

Copyright Statement

The authors confirm that they, and/or their company or organization, hold copyright on all of the original material included in this paper. The authors also confirm that they have obtained permission, from the copyright holder of any third party material included in this paper, to publish it as part of their paper. The authors confirm that they give permission, or have obtained permission from the copyright holder of this paper, for the publication and distribution of this paper as part of the ICAS proceedings or as individual off-prints from the proceedings.